Suboptimal T-cell receptor signaling compromises protein translation, ribosome biogenesis, and proliferation of mouse CD8 T cells

Thomas C. J. Tan[a], John Knight[b,1], Thomas Sbarrato[b,2], Kate Dudek[b], Anne E. Willis[b], and Rose Zamoyska[a,3]

[a]Institute of Immunology and Infection Research, Ashworth Laboratories, University of Edinburgh, Edinburgh EH9 3FL, United Kingdom; and [b]Medical Research Council Toxicology Unit, Leicester LE1 9HN, United Kingdom

Edited by Douglas R. Green, St. Jude Children's Research Hospital, Memphis, TN, and accepted by Editorial Board Member Arthur Weiss June 13, 2017 (received for review January 23, 2017)

Global transcriptomic and proteomic analyses of T cells have been rich sources of unbiased data for understanding T-cell activation. Lack of full concordance of these datasets has illustrated that important facets of T-cell activation are controlled at the level of translation. We undertook translatome analysis of CD8 T-cell activation, combining polysome profiling and microarray analysis. We revealed that altering T-cell receptor stimulation influenced recruitment of mRNAs to heavy polysomes and translation of subsets of genes. A major pathway that was compromised, when TCR signaling was suboptimal, was linked to ribosome biogenesis, a rate-limiting factor in both cell growth and proliferation. Defective TCR signaling affected transcription and processing of ribosomal RNA precursors, as well as the translation of specific ribosomal proteins and translation factors. Mechanistically, IL-2 production was compromised in weakly stimulated T cells, affecting the abundance of Myc protein, a known regulator of ribosome biogenesis. Consequently, weakly activated T cells showed impaired production of ribosomes and a failure to maintain proliferative capacity after stimulation. We demonstrate that primary T cells respond to various environmental cues by regulating ribosome biogenesis and mRNA translation at multiple levels to sustain proliferation and differentiation.

CD8 T cell | translation | polysome profile | ribosome biogenesis | signaling

Naive T cells exist for many years in the circulation, in an extremely metabolically indolent state, synthesizing little RNA and protein (1). At this stage, their survival is regulated by tonic signaling from growth factors and antigen-specific T-cell receptors (TCRs). Once triggered by engagement of the TCR, naive T cells rapidly turn on gene transcription and protein synthesis and increase in volume over a 24-h period to become large blasting cells, before commencing division. This size increase is accompanied by a 17-fold increase in production of RNA polymerases I and III, consistent with a substantial increase in ribosome biogenesis that is required to produce the proteins essential for T-cell proliferation and differentiation (1). At the peak of a response, the CD8 subpopulation of T cells divides with a doubling time of as little as 2 h (2) until antigen is cleared, whereupon the majority of T cells die and the remainder revert once more to a resting, memory cell state.

The extent of TCR triggering is linked to T-cell fate. Strong agonist ligands stimulate maximal clonal proliferation, differentiation to effector function, and the development of memory cells whereas weaker ligands drive less proliferation and effector differentiation, yet still allow differentiation to memory cells (3). Although changes in gene transcription influence these cell fates, there is also substantial control regulated at the level of translation. Particular groups of proteins, such as effector cytokines, chemokines, and chemokine receptors, have been shown to be highly regulated posttranscriptionally in T cells (4). For example, primed T cells accumulate a repertoire of effector mRNAs that are made into proteins only upon secondary TCR stimulation (5), restricting production of potent cytokines to the site of pathogen reencounter. Many mRNAs have been shown to undergo shortening of their 3′ UTRs after several rounds of T-cell proliferation (6), suggesting that control of translation pertains to a number of mRNAs and is important for the function of T cells. These data indicate that, upon activation, T cells prioritize translation of specific mRNAs, in addition to regulating more global production of proteins, although the mechanisms by which T cells exert this discrimination is not well-understood.

In mammalian cells, a rate-limiting step in controlling growth and proliferation is the availability of ribosomes (7, 8). Ribosome biogenesis is a complex and tightly regulated process requiring the activity of all three RNA polymerases and the synthesis and coordinated assembly of multiple proteins and specific rRNAs (9). Thus, ribosome biogenesis requires a large bioenergetic investment (10) and is actively maintained in continuously proliferating, transformed cells and cell lines. In cells that are in a resting state (for example, serum-starved fibroblasts), the number of ribosomes is lower, increasing approximately two- to threefold upon resumption of active growth (11). Activated T cells devote

Significance

Optimal antigenic stimulation through T-cell receptors is required by T lymphocytes to exert full expansion, effector functions, and memory cell differentiation. Suboptimal TCR stimulation influences both transcription of genes and synthesis of subsets of proteins in a nonconcordant manner. Detailed polysome profiling revealed that weakly activated cells prioritized mRNA translation so that specific transcripts were translationally sequestered. Strikingly, ribosome biogenesis was compromised at both transcriptional and translational levels after weak stimulation, which still allowed the cells to undergo initial cell division, but proliferation was not sustained. Our work has demonstrated that T cells respond to environmental signals and use specific components of the translation machinery to regulate the translation of activation-dependent mRNAs.

Author contributions: T.C.J.T., A.W., and R.Z. designed research; T.C.J.T. performed research; J.K. and K.D. contributed new reagents/analytic tools; T.C.J.T., J.K., and T.S. analyzed data; and T.C.J.T. and R.Z. wrote the paper.

The authors declare no conflict of interest.

This article is a PNAS Direct Submission. D.R.G. is a guest editor invited by the Editorial Board.

Data deposition: The data reported in this paper have been deposited in the Gene Expression Omnibus (GEO) database, https://www.ncbi.nlm.nih.gov/geo (accession nos. GSE84781 and GSE84856).

[1]Present address: The CRUK Beatson Institute, Bearsden, Glasgow G61 1BD, United Kingdom.

[2]Present address: Adhesion and Inflammation Lab UM 61, Aix Marseille Université, Marseille, F-13288, France; Inserm, UMR_S 1067, Marseille, F-13288, France; and CNRS, UMR 7333, Marseille, F-13288, France.

[3]To whom correspondence should be addressed. Email: Rose.Zamoyska@ed.ac.uk.

This article contains supporting information online at www.pnas.org/lookup/suppl/doi:10.1073/pnas.1700939114/-/DCSupplemental.

significant bioenergetic investment into ribosome biogenesis. Mass spectroscopy analysis of proteins present in CD8 T cells during their peak expansion phase showed that ~10% of identified proteins contributed to ~85% of the total proteome and that the majority of these highly abundant proteins are involved in ribosome biogenesis (12). The purpose of the current study was to investigate how T cells manage the switch from inertia in the resting state to rapid expansion and differentiation after activation, with regard to their ribosome capacity, and their ability to translate the mRNAs required for these processes.

To investigate how T cells prioritized translation upon activation, we stimulated naive OT-1 TCR transgenic $CD8^+$ T lymphocytes with defined peptide ligands in vitro. The strength of TCR activation was manipulated either genetically, by turning off Lck expression, or with weak peptide ligands. By combining these manipulations with global polysome profiling, we identified specific gene subsets that are translationally regulated by TCR-dependent signaling pathways. In particular, we discovered that, upon TCR activation, ribosome biogenesis is controlled at multiple levels: in rRNA precursor transcription and processing and in the translation of mRNAs involved in these processes. Weak TCR signals failed to sustain ribosome biogenesis, in direct correlation with their ability to produce IL-2 and thus maintain the abundance of Myc protein. The data show that T cells respond to TCR stimulation in a dynamic fashion by regulating the production, and therefore the availability, of functional ribosomes in the cell, with consequent influences on both global and specific protein translation and proliferative capacity.

Results

TCR Signaling Regulates Both Total Protein Synthesis and Specific mRNA Translation. Engagement of the TCR with peptide:MHC triggers a number of biochemical changes initiated by activation of the Src family kinases (SFKs), inhibition of which aborts T-cell activation (13). Of the two major SFK members in T cells, $p56^{Lck}$ (Lck) and $p59^{Fyn}$ (Fyn), Lck was shown to be the more influential for setting the threshold of T-cell triggering (14). In primary T cells in the absence of Lck, Fyn can substitute to some extent so that cells become activated, but through a more restricted set of signaling pathways (15). Removal of Lck is a useful means of manipulating TCR signal strength; therefore, we used $Lck^{-/-}$ mice expressing a tetracycline-inducible Lck transgene to abrogate Lck expression in peripheral T cells (16). Mice were maintained on doxycycline (Dox)-containing food from birth to drive expression of Lck, which is required for T-cell differentiation and establishment of the naive peripheral T-cell pool. Dox was removed from food 7 to 10 d before harvest of lymph nodes, which allowed sufficient time for any residual Lck protein in the cells to decay (17).

OT-1 Rag-$1^{-/-}$ T cells and $Lck^{-/-}$ OT-1 Rag-$1^{-/-}$ T cells (hereafter referred to as WT and $Lck^{-/-}$ T cells) were stimulated for 24 h with optimal concentrations of SIINFEKL (N4) peptide to activate all cells, assessed by up-regulation of activation protein, CD69, measured by FACS (Fig. 1*A*). At 24 h, T cells had also up-regulated transcription and translation, doubling their protein content (Fig. 1*B*), but had not entered division. Comparison of forward scatter (FSC) plots, a surrogate for cell size, showed that WT cells were ~14% larger than $Lck^{-/-}$ cells (Fig. 1*A*), which correlated with more total protein in the former by ~17% (Fig. 1*B*). We saw that the abundance of CD25 protein measured on WT cells [by mean fluorescence index (MFI)] was significantly higher than on $Lck^{-/-}$ T cells whereas the MFI of CD69 was comparable between the two genotypes (Fig. 1*A*), suggesting that specific proteins may be differentially regulated in the absence of Lck.

To understand the mechanism regulating CD25 expression, we assessed transcription, translation, and protein abundance of both CD25 and CD69 in activated WT and $Lck^{-/-}$ T cells (Fig. 1*C*).

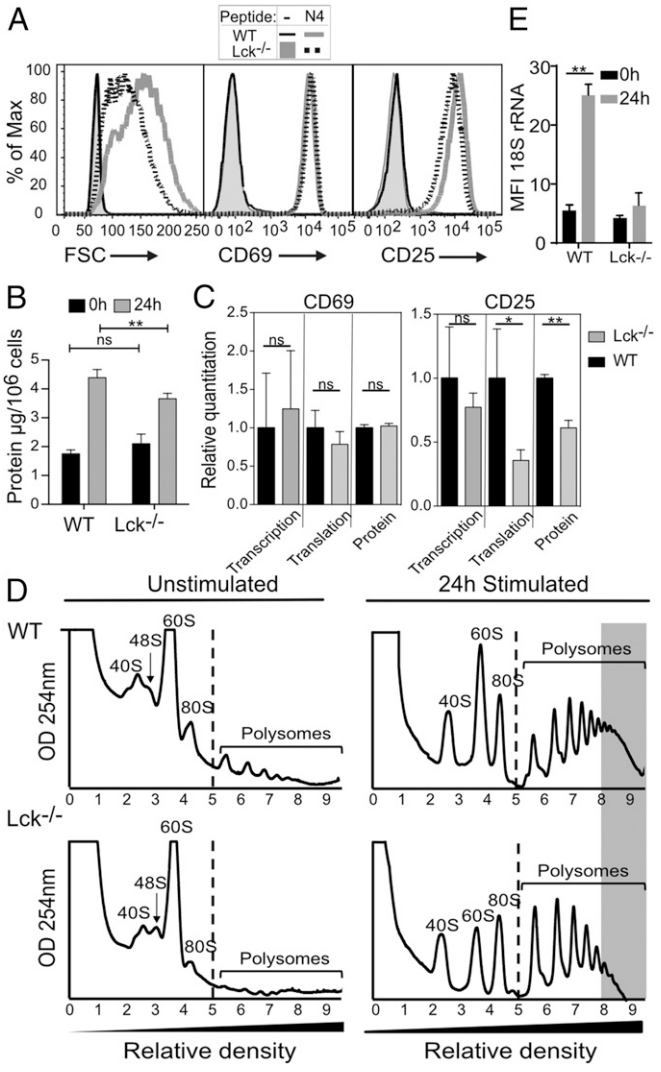

Fig. 1. Reduced translation of specific activation-associated genes together with decreased total protein synthesis in the absence of Lck-mediated TCR signaling. Unstimulated naive and SIINFEKL (N4) peptide-stimulated OT-1 (WT) and OT-1 $Lck^{-/-}$ ($Lck^{-/-}$) CD8 T cells were compared after 24h for (*A*) increased size, measured by forward scatter profiles (FSC), and expression of activation markers CD69 and CD25 by FACS; (*B*) total protein content quantified by BCA assay ($n = 4$, $^{**}P < 0.01$, two tailed t test); and (*C*) relative quantitation of CD69 and CD25 transcription by RT-qPCR of total mRNA, translation, by RT-qPCR of polysome-associated and unassociated mRNAs, and protein assessed by mean fluorescence index (MFI) values from FACS analysis (Transcription, $n = 3$; Translation, $n = 4$; Protein, $n = 7$; $^{*}P < 0.05$, $^{**}P < 0.01$, two-tailed t test). (*D*) Global sucrose gradient profiles of stimulated and unstimulated WT and $Lck^{-/-}$ cells. Shaded area denotes mRNAs associated with more than six ribosomes. For each time point, lysates were extracted from equal cell numbers and analyzed on the same day to allow direct comparison of profiles. (*E*) Mean fluorescent intensity of 18S rRNA in stimulated and unstimulated WT and $Lck^{-/-}$ cells, measured by flow-FISH ($n > 4$, $^{**}P < 0.01$, two-tailed t test). ns, nonsignificant.

Transcription was measured from total mRNA by microarray and validated by quantitative RT-PCR (RT-qPCR), whereas translation was measured by sucrose gradient fractionation of the cytoplasmic RNA to separate translationally active mRNAs (polysome-bound, Fig. 1*D*, fractions 5 to 9) from repressed transcripts (subpolysomal, Fig. 1*D*, fractions 1 to 4). Translational activity of a gene was defined as the abundance of its mRNA in the polysomal fraction divided by that in the subpolysomal fraction. Protein abundance was taken from MFI values measured by

FACS. Fig. 1*C* shows that total mRNA abundance for each marker was equivalent in WT and Lck$^{-/-}$ T cells. Translation of CD69 was also equivalent between the two cell types because its mRNA was similarly distributed between subpolysome and polysome fractions. In contrast, CD25 mRNA was significantly underrepresented in polysomes in Lck$^{-/-}$ T cells, which correlated with reduced protein expression by FACS analysis. Therefore, CD25 protein production seems to be regulated at the level of translation in cells lacking Lck rather than by reduced transcription of the gene.

TCR Signals Regulate Expression of Multiple Genes at the Level of Translation. To obtain a more global appreciation of which proteins in CD8 T cells might be regulated at the level of translation after suboptimal stimulation, we undertook a microarray analysis of ribosome-associated mRNA. First, we compared ribosomal profiles obtained from naive T cells, which showed an abundant free 60S peak and an accumulation of 48S preinitiation complex, indicating very little translation initiation occurred in naive T cells (Fig. 1*D*). Additionally there was an absence of polysome-associated peaks, suggesting limited protein translation, which was consistent with the metabolically inert nature of these cells. After stimulation with antigen, WT T cells dramatically upregulated active translation, indicated by a reduced free 60S peak and an increase in mRNA associated with polysomes. There was a shift in total distribution of material in the subpolysome fraction from >85% in naive WT T cells to ~50% in activated T cells. The fractions that contained the heaviest polysomes (Fig. 1*D*, shaded area, fractions 8 and 9) and thus the most actively translated mRNAs represented a substantial proportion of the total cytoplasmic RNA species in the activated WT cells (ratio of heavy:light polysomes 0.53 ± 0.3). In contrast, stimulated Lck$^{-/-}$ cells had smaller 40S, 60S, and 80S peaks, suggesting fewer functional ribosomes, which might result in inefficient translation initiation. We confirmed this finding by directly quantitating the level of 18S rRNA per cell using flow-FISH (Fig. 1*E*), which showed more than threefold reduction in 18S rRNA abundance in Lck$^{-/-}$ cells ($n \geq 4$, $P < 0.01$, two-tailed *t* test). Additionally the sucrose gradient analysis showed in Lck$^{-/-}$ T cells that the majority of translated mRNAs were located in the lighter 3- to 6-polysomal region and that the ratio of heavy:light polysomes was significantly lower (0.09 ± 0.06), indicating a reduction in overall translation activity in these cells.

Actively translated mRNAs in stimulated cells were identified by polysome association of individual genes, measured by two-colored microarray. Signals produced by RNA extracted from the polysomal region (Fig. 1*D*) were normalized against the signals in the subpolysomal fractions (Fig. 1*D*, left of the broken line), for WT and Lck$^{-/-}$ T cells. These normalized values were expressed as a fold-change in polysome association between the two cell types. Of 19,282 unique expressed microarray probes, 4,535 (23.5%) were significantly reduced in polysome association ($P < 0.05$, RankProd test) in stimulated Lck$^{-/-}$ cells compared with WT cells (https://www.ncbi.nlm.nih.gov/geo/query/acc.cgi?acc=GSE84781). When analyzed together with total transcript microarrays derived from the same biological samples (https://www.ncbi.nlm.nih.gov/geo/query/acc.cgi?acc=GSE84856), it was found that gene regulation at the level of transcription correlated poorly to regulation at the translation level ($R^2 < 0.004$) (Fig. 2*A*). Using a RankProd *P* value threshold of 0.05, a three-way Venn analysis was undertaken that showed that there were multiple transcripts significantly down-regulated in translation, up-regulated in transcription, and down-regulated in transcription in stimulated Lck$^{-/-}$ cells compared with WT cells (Fig. 2*B*). RT-qPCR validations of sucrose gradient fractions were performed on an additional 13 transcripts related to T-cell activation in addition to CD69 and CD25, which confirmed that 11 of the 15 transcripts tested were translationally repressed in the absence of Lck signals (Fig. 2*C* and extended data in Table S1). Genes subjected to uncoupled transcription and translation regulation (white areas in the Venn diagram in Fig. 2*B*) were isolated and analyzed by functional clustering using WebGestalt (18, 19). Notably, a specific subset of abundant genes associated with ribosome biogenesis were translationally repressed in Lck$^{-/-}$ cells (Fig. 2*D* and Table 1), suggesting that signals downstream of Lck were specifically involved in regulating their translation. Given that ribosome biogenesis is essential to produce sufficient ribosomes for maintaining translation during this phase of active T-cell expansion and differentiation, we investigated further how it was regulated in CD8 T cells.

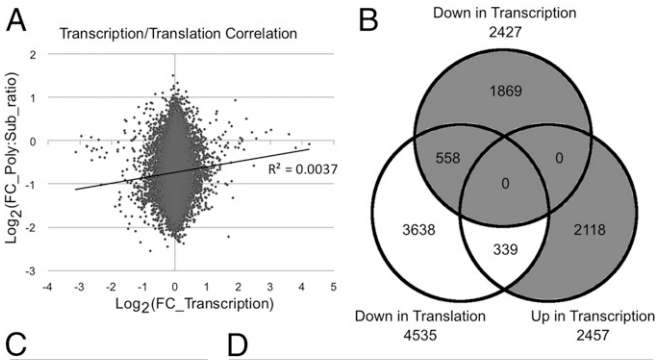

C

Decreased	Unchanged
Il2ra (CD25)	*CD69*
BclxL	*Socs1*
Gadd45b	*Socs3*
Myc	*Eefg1*
Pik3cd	*Eef2*
IFNg	
Ifngr1	
Il2rb	
Cish	
Sfpq	

D

	KEGG Pathway	No. of probes	Adj.Pvalue
	Metabolic pathways	281	4.79E-121
	Oxidative phosphorylation	74	2.58E-57
	Spliceosome	61	9.40E-43
	Protein processing in endoplasmic reticulum	62	1.30E-37
	Proteasome	34	1.01E-34
	RNA transport	55	2.78E-30
*	**Ribosome biogenesis in eukaryotes**	**38**	**2.70E-26**
	Lysosome	39	1.19E-20
	Ubiquitin mediated proteolysis	39	2.21E-18
	mRNA surveillance pathway	28	6.25E-14
	Endocytosis	41	1.24E-12
	RNA polymerase	16	1.69E-12
	RNA degradation	23	2.42E-11
	Cell cycle	29	5.18E-11
	T cell receptor signaling pathway	26	3.74E-10
	DNA replication	15	1.37E-09
	Regulation of actin cytoskeleton	36	1.66E-09
	Nucleotide excision repair	16	3.65E-09
	MAPK signaling pathway	38	6.09E-08
	Focal adhesion	29	4.45E-06
	Protein export	11	1.40E-05
	mTOR signaling pathway	13	8.00E-05
	Basal transcription factors	9	0.0042
	Apoptosis	14	0.005

Fig. 2. Lck signals regulate translation of groups of mRNAs in stimulated T cells. (*A*) Correlation between Lck-dependent transcriptional and translational regulation in 24 h activated CD8 T cells, measured by microarrays using total (GEO accession no. GSE84856) or sucrose-fractionated RNA (GEO accession no. GSE84781), respectively ($n = 4$). (*B*) Venn overlay of differentially transcribed and translated microarray probes between WT and Lck$^{-/-}$ cells. Shaded areas indicate genes regulated by transcription; white areas indicate genes subjected to uncoupled transcription and translation control. (*C*) Genes validated by RT-qPCR whose translation is down-regulated or unchanged by the absence of Lck signals after 24-h stimulation with N4 peptide. For full details of analysis, see Table S1. (*D*) A representation of KEGG enrichment analysis of genes subjected to uncoupled regulation (white area in the Venn analysis) using WebGestalt with Bonferroni correction. The ribosome biogenesis pathway, which was followed up in this study, is indicated in bold and with an asterisk.

TCR Signaling Regulates Alternate Transcription and Processing of rRNA Precursors. Ribosome biogenesis is a highly regulated process involving multiple molecular components, including rRNAs, ribosomal proteins, associated factors, and small nuclear RNAs. In the case of rRNAs, they are transcribed as precursor molecules, which are processed by cleavage in the nucleus (as outlined in Fig. 3*A*) before export to the cytoplasm (9).

To understand how ribosome production is regulated in T cells, we investigated the time course of ribosome biogenesis in OT-1 WT T cells by examining on Northern blots the appearance of pre-18S rRNA precursors in cells after activation, using an ITS-1 rRNA small subunit precursor probe. Fig. 3*B* shows that naive resting T cells (0 h) had a predominant 47/45S, 30S, and

Table 1. Specific subset of highly expressed genes in the ribosome biogenesis pathway is translationally regulated by TCR signals

Gene	Transcription level, %	Fold change in transcription	RankProd Test (transcription)	Fold change in polysome association	RankProd Test (translation)
			rDNA gene transcription		
Tcof1	90.05	1.03	n.s.	−4.01	**
			Early precursor processing		
Nop58	90.45	1.04	n.s.	−3.58	**
Csnk2b	94.38	1.04	n.s.	−3.33	**
Nop10	93.75	−1.00	n.s.	−3.28	**
Fbl	91.92	1.03	n.s.	−3.09	**
Wdr36	68.68	−1.01	n.s.	−3.08	**
Gar1	95.26	1.11	n.s.	−3.02	**
Nhp2	97.70	1.00	n.s.	−3.01	**
Taf9	85.98	1.15	n.s.	−3.00	**
Cirh1a	89.27	1.01	n.s.	−2.97	**
Dkc1	66.73	−1.00	n.s.	−2.96	**
			40S or 60S subunit maturation		
Xrn2	76.63	1.01	n.s.	−3.04	**
Utp14a	69.71	1.43	**	−2.89	**
Pop5	95.30	−1.05	n.s.	−3.72	**
Emg1	82.86	−1.02	n.s.	−2.94	**
Pop7	90.72	−1.07	n.s.	−2.91	**
Eif6	91.99	−1.02	n.s.	−3.20	**
			Ribosomal protein		
Rpl4	96.92	1.19	n.s.	−2.45	*
Rpl36al	94.28	1.13	n.s.	−2.26	*
Rps27l	96.87	−1.15	n.s.	−2.57	*
			Nuclear export		
Rasl2-9	95.41	−1.09	n.s.	−3.16	**
Nxt1	87.95	−1.04	n.s.	−3.51	**
Xpo1	85.70	−1.13	n.s.	−3.01	**

Transcription and polysome association were measured from total RNA or polysomal/subpolysomal RNA extracted from WT and $Lck^{-/-}$ cells ($n = 4$) stimulated with SIINFEKL peptide for 24 h. The transcription level percentile for each gene was calculated based on the 19,282 unique expressed probes. All genes presented in the table were selected and annotated according to their abundance and their known roles in rRNA transcription, processing, or nuclear export. The fold changes are expressed as the level in $Lck^{-/-}$ cells versus WT cells. Statistical significance: $*P < 0.05$, $**P < 0.01$, RankProd test; n.s., nonsignificant.

21S precursor rRNA species, but little of the other sized intermediates, particularly the final 18S-E precursor species generally seen in actively growing cells. The abundance of 30S rRNA suggested a failure of downstream pre-rRNA cleavage. The presence of 21S and scarcity of 26S indicated that naive T cells preferentially used the major 30S-21S cleavage pathway without the activation of the alternative 30S-26S-21S pathway (20) whereas the paucity of 18S-E suggested that the cleavage process after 21S was hindered.

Upon stimulation with cognate peptide antigen, rRNA processing increased, shown by a twofold decrease in the band intensity of 30S and 21S at 2 h and 4 h, respectively (Fig. 3*B*). A concomitant increase in rRNA transcription upon activation was indicated by a twofold increase in the precursor 45/47S band intensity at 2 h. By 8 h of Ag stimulation, the abundance of total ITS-1 signal increased by 2.2-fold over naive cells, as did bands corresponding to late precursors, 26S and 18S-E, suggesting that an efficient rRNA processing mechanism was present for both major and alternative cleavage pathways. By 24 h, total ITS-1–containing pre-rRNAs were >12.5 times more abundant than in naive cells. Similar results were obtained with an ITS-2 probe that measured pre-5.8S and pre-28S rRNA precursors (Fig. 3*C*).

Precursor product relationships are more clearly ascertained by pulse–chase approaches rather than by snapshots of rRNA processing at particular times after stimulation. However, the inert nature of naive T cells means that they do not incorporate appreciable amounts of radiolabel before they are activated. In Fig. 3*D* (0 h), naive T cells were incubated with ^{32}P for 1 h before sampling; however, no incorporation of label into rRNA precursors was visible on the gel. Labeled rRNA species began to be visible by 1 h after stimulation, and incorporation then proceeded exponentially, with a fourfold increase by 4 h and 16-fold by 8 h (Fig. 3 *D* and *E*). ^{32}P incorporation in mature 18S and 28S species was detected from 1 h, and, by 2 h, equimolar ratios of mature rRNAs and pre-rRNAs were observed (longer exposure in Fig. 3*D*, *Right*), indicating that intact pre-rRNA processing mechanisms were present at this early stage of activation in WT cells because there was no visible accumulation of precursors compared with their cleavage products.

Weak Alternate Peptide Ligands Stimulate Ribosome Biogenesis Poorly. Experimental removal of Lck by genetic manipulation is a useful tool to probe signals downstream of the TCR and will mimic the status of aging lymphocytes that lose expression of Lck (21, 22). In Lck-sufficient T cells, Lck activation upon TCR binding can be influenced also by the extent and duration of coreceptor recruitment, which happens when T cells are stimulated by altered peptide ligands with low affinities (23–25). A consequence of stimulation by altered peptide ligands is that the expansion potential of T cells is curtailed compared with that induced by strong agonist ligands (3). Therefore, we were interested to compare ribosome biogenesis between $Lck^{-/-}$ T cells stimulated with strong peptides and Lck-sufficient WT T cells that were stimulated with weak agonist antigens. A number of variant peptides of OVA have been described that have amino acid substitution of the forth residue, which do not change

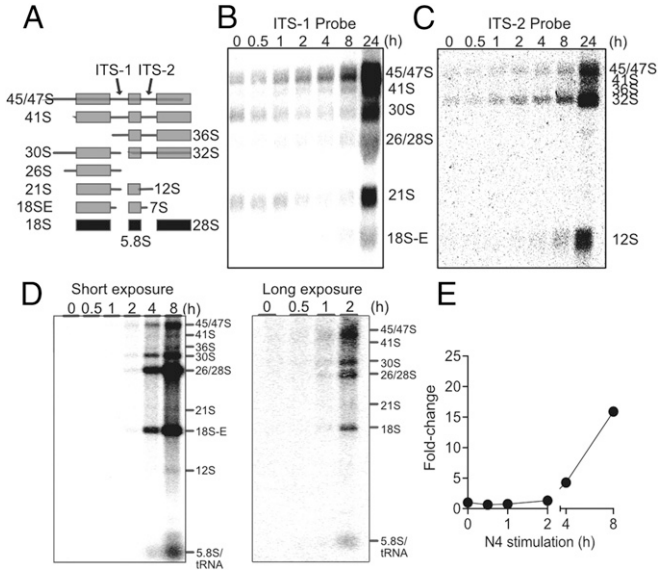

Fig. 3. T-cell activation involves both transcription and processing of ribosomal RNA precursors. (*A*) Schematic diagram of mammalian rRNA precursors. Boxed regions correspond to the locations of mature 18S, 5.8S, and 28S rRNA. Regions detectable by the ITS-1 and ITS-2 probes are marked with arrows. (*B*) rRNA precursors in total RNA extracted from WT OT-1 peripheral T lymphocytes activated with N4 peptide, visualized by Northern blot hybridized with an ITS-1 probe (for small subunit precursors). Each lane was loaded with RNA from an equal number of cells. (*C*) Rehybridization of the membrane in *B* with an ITS-2 probe (for large subunit rRNA precursors). (*D*) Naive T cells were preincubated for 1 h with ^{32}P before addition of N4 peptide (0 h). Incorporation of ^{32}P into rRNAs was followed by sampling over an 8-h time course. Longer exposure of ^{32}P incorporation for 0-h, 0.5-h, 1-h, and 2-h samples is shown on the *Right*. (*E*) Fold change in the rate of ^{32}P incorporation at various time points after N4 peptide stimulation, relative to the rate in naive cells. Representative results of three independent experiments are shown.

peptide association with MHC, but alter the dwell time of interaction with the OT-1 TCR and therefore the efficacy with which they stimulate CD8 T cells (3, 26). Activation of WT OT-1 T cells with the variant ligand SIIGFEKL (G4) was compared with WT and Lck$^{-/-}$ OT-1 T cells activated with the strong agonist peptide SIINFEKL (N4), with regard to their ability to stimulate ribosome biogenesis.

First, we compared T-cell activation by phospho-flow analysis to benchmark similarities and differences in signal transduction between WT OT-1 T cells stimulated with strong, N4, and weak, G4, peptide agonists and N4-stimulated Lck$^{-/-}$ T cells (Fig. 4*A*). WT N4-stimulated T cells were most activated, with the highest proportion of pERK^{+} and pRPS6^{+} cells and the greatest mean fluorescent intensity of pAKT and p4EBP1 (Fig. 4*A*). Lck$^{-/-}$ T cells stimulated with N4 peptide had an intermediate profile, between N4- and G4-stimulated WT cells, for up-regulation of activation markers and increase in cell size. WT T cells stimulated with G4 peptide showed the weakest response, indicating that this stimulus affected activation more profoundly than simply removing Lck. It is likely that G4 stimulation of WT cells also failed to fully stimulate the PI3K pathway, given the reduced activation of AKT. Despite the poor phosphorylation of these signaling molecules, all G4-activated WT cells up-regulated CD25 and CD69 by 24 h after stimulation, although to a lesser extent than WT N4-stimulated cells. Additionally G4-stimulated cells remained considerably smaller than WT cells stimulated with N4 peptide (Fig. 4*B*, FSC histograms).

To ask how stimulation with weak peptide influenced ribosome biogenesis, we compared rRNA precursors by Northern blot analysis using the ITS-1 probe (Fig. 4*C*). Because the level of pre-rRNA in unstimulated cells was very low (Fig. 3*B*), the majority of pre-rRNA present at 24 h will have been synthesized de novo after cell activation, and therefore the relative quantity of individual ITS-1–containing pre-rRNA species should reveal

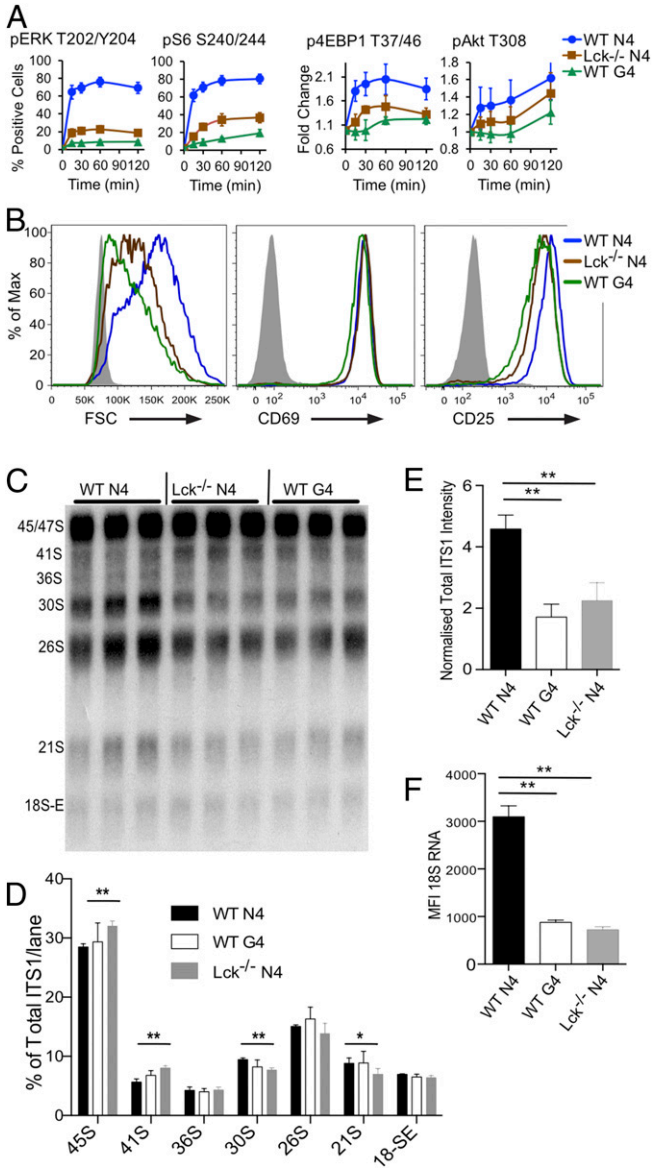

Fig. 4. Weak TCR signals alter TCR signaling and regulate pre-18S rRNA transcription and processing. WT and Lck$^{-/-}$ OT-1 T cells were stimulated with strong agonist SIINFEKL (N4) peptide, or WT T cells were stimulated with weak agonist SIIGFEKL (G4) peptide. (*A*) pERK (pT202/Y204), pRPS6 (pS240/244), p4EBP1 (T37/46), and pAkt (pT308) were measured by FACS after a short stimulation time course (0 to 2 h) ($n \geq 4$). (*B*) FSC and expression of activation markers CD69 and CD25 in stimulated populations at 24 h were compared with nonstimulated controls (shaded histograms). (*C*) Relative abundance of ITS-1 rRNA precursors in total RNA extracted from three biological replicates of WT and Lck$^{-/-}$ cells stimulated with N4 peptide and WT cells stimulated with G4 peptide for 24 h. Equal quantities of total RNA were loaded in each lane. (*D*) Quantification of the relative ^{32}P intensity of each precursor normalized to total ITS-1 signal per lane ($n = 3$). (*E*) Total ITS-1 rRNA precursor signal intensity per lane normalized to cell number loaded ($n = 3$). (*F*) Mean fluorescent intensity of 18S rRNA in stimulated and unstimulated WT and Lck$^{-/-}$ cells, measured by flow-FISH ($n \geq 4$). Error bars correspond to 1 SD of the mean. *$P < 0.05$, **$P < 0.01$, two-tailed *t* test.

differences in the processing rate between samples. Quantification revealed that Lck$^{-/-}$ N4-stimulated T cells possessed a significantly higher proportion of early 45/47S and 41S species, together with lower proportion of later 30S and 21S rRNA species, whereas the distribution of these precursors in WT cells stimulated with N4 or G4 did not reveal significant differences (Fig. 4*D*). Overall, WT N4-stimulated cells had an approximately twofold increase in total ITS-1 signal per cell compared with both Lck$^{-/-}$ N4-stimulated and WT G4-stimulated T cells (Fig. 4*E*). Equivalent results were found with an ITS-2 probe, which showed that 41S and 36S were significantly enriched, while 32S species were reduced, in N4-stimulated Lck$^{-/-}$ compared with N4-stimulated WT cells whereas WT cells stimulated with either N4 or G4 were more comparable (Fig. S1).

Together, the data showed that impaired TCR signals, such as G4 stimulation of WT cells or N4 stimulation of Lck$^{-/-}$ cells, reduced the overall abundance of ITS-1 and ITS-2 rRNA species, most likely by reducing transcription; however, in the absence of Lck, there was also some evidence of defective processing of these precursors, which was less apparent in G4-stimulated WT cells (Fig. 4*D*). To investigate ribosome availability in these cells, we used flow-FISH to measure total 18S rRNA per cell (Fig. 4*F*). There was approximately a threefold drop in total 18S rRNA in both WT G4-stimulated and Lck$^{-/-}$ N4-stimulated cells compared with WT N4-stimulated cells at 24 h, confirming a reduction of ribosome abundance after weak stimulation.

From the previous experiments, we concluded that there was a significant decline in pre-rRNA transcription and processing in T cells receiving weak signals. In Lck$^{-/-}$ cells, this decline limited the functional ribosomes available for translation and contributed to the global shift in the polysome profiles. We also examined translation factor abundance to ask whether it might also account for the altered polysome profiles. Analysis by Western blotting showed no difference in the abundance of eIF2α, eIF4A2, eIF5A, and eEF2 at 24 h; however, there was a 30% reduction in expression of eIF6 in Lck$^{-/-}$ T cells (Fig. 5*A*). FACS analysis confirmed that the abundance of eIF5A and eIF6 increased by 3.6-fold and 23-fold, respectively, after 24 h of TCR stimulation and that the level of eIF6 was significantly lower in activated Lck$^{-/-}$ cells compared with WT cells (Fig. 5*B*). Together, these data suggested that several elements, including eIF6 availability, are likely to have contributed to both global and specific gene translation during early T-cell activation.

Inefficient Ribosome Biogenesis in Lck$^{-/-}$ Cells Causes Loss of Proliferative Capacity. We examined what the consequences of reduced ribosome production in Lck$^{-/-}$ cells might be on the ability of the cells to trigger and sustain proliferation. Using Ki67, to indicate active cell cycle, together with Hoechst 33342 staining, we compared WT and Lck$^{-/-}$ T cells stimulated with N4 peptide (Fig. 6 *A* and *B*). At 24 h after stimulation, a substantial proportion of WT cells were in S phase whereas the majority of Lck$^{-/-}$ cells were still in G0/1 phase, indicating a delay in commencing DNA replication. Both cell types showed comparable distribution between G0/1, S, and G2/M at 48 h (Fig. 6*B*). However, the proliferation of Lck$^{-/-}$ cells collapsed by 72 h, with significantly reduced Ki67^{+} population and very few cells in S and G2/M phase cells compared with WT cells. A significantly greater proportion of dead cells, characterized on the basis of changes to FSC and side scatter (SSC) (Fig. 6*C*), were recovered from the 72-h Lck$^{-/-}$ cultures compared with the WT cultures. This difference was not present at 48 h, indicating that the decrease in cell survival occurred after the onset of cell proliferation. Overall, weakly stimulated cells proliferated less (Fig. 6*E*) and had greatly reduced live cell recovery (Fig. 6*F*).

Together, the data indicated that full agonist stimulation, as provided to WT cells by N4 peptide, is required to optimize translation during early CD8 T-cell activation and to sustain survival and proliferation at later stages of the response. Only these cells seemed to have enough ribosome sufficiency to be able to sustain active rapid proliferation over multiple days.

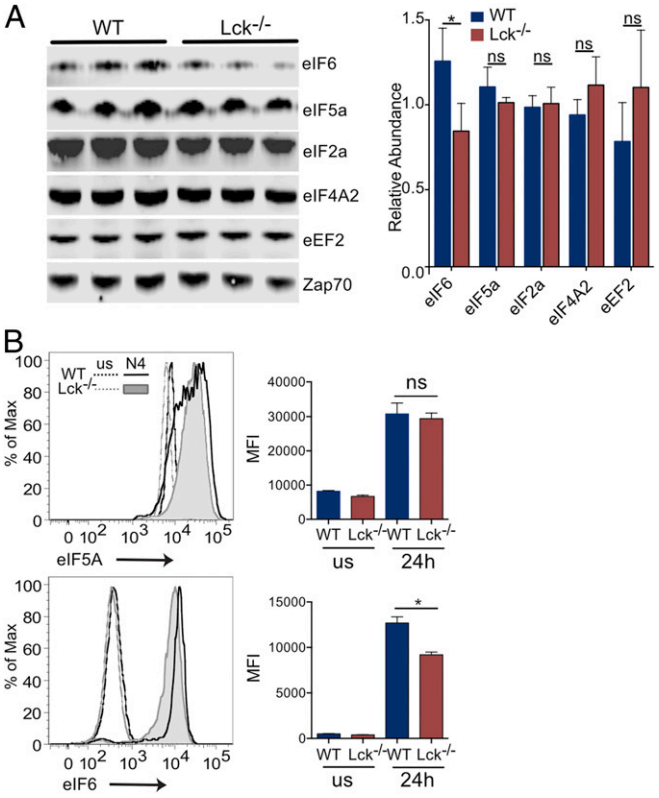

Fig. 5. Stimulation of T cells in the absence of Lck alters the abundance of specific proteins involved in translation. (*A*) OT-1 T Cells were stimulated with N4 peptide for 24 h, and (*Left*) whole cell lysates from equal numbers of cells were loaded per lane. Western blots were probed sequentially with the indicated Abs and were normalized against ZAP-70 as a loading control (n = 3). *Right* shows the quantitated normalized values. (*B*) The abundances of eIF5A and eIF6 were confirmed by intracellular FACS staining (*Left*) of unstimulated (us) and 2-h N4-stimulated T cells. (*Right*) Bar charts represent the mean fluorescence intensity in each sample (n = 3). Error bars correspond to 1 SD of the mean. *P < 0.05, **P < 0.01, two-tailed t test. ns, nonsignificant.

Exogenous IL-2 Rescues Ribosome Biogenesis in Weakly Stimulated T Cells. IL-2 is a key cytokine providing signals required for proliferation and survival of T cells during activation (27). Transcription of *Il2* mRNA is regulated by activation-induced factors, such as NFAT (28) and AP1 (29), and, in weakly activated T cells, either in the absence of Lck (15) or with low affinity antigenic stimulation (Fig. 7*A*), production of IL-2 is impaired. To ask whether lack of IL-2 underpinned the TCR-dependent regulation of ribosome biogenesis, we activated WT cells with G4 antigen in the presence or absence of exogenous IL-2 in culture and monitored proliferation and ribosome production in these cells.

Cell cycle analysis revealed that addition of IL-2 to the culture rescued the collapse of cell division seen in G4-stimulated cells at 72 h (Fig. 7*A*), with the percentage of G0/1, S, and G2/M cells comparable with WT cells without exogenous IL-2. Because IL-2 is required for sustained expression of Myc in T cells (27, 30) and many key genes involved in rRNA processing and ribosome assembly are targets of Myc regulation (31, 32), we measured by FACS the intracellular level of Myc and one of its targets, fibrillarin, a site-specific methyltransferase required for pre-rRNA processing. Initially Myc expression in T cells is driven exclusively by TCR engagement (30), and, at 24 h, Myc was upregulated more strongly in N4-stimulated than in G4-stimulated

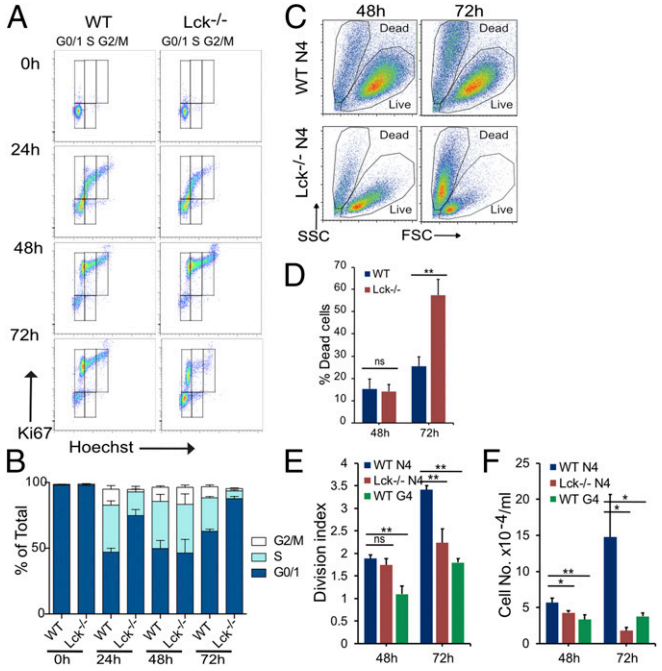

Fig. 6. Optimal TCR stimulation and ribosome production are required for T-cell survival and proliferation. (*A*) Analysis of cell cycle and proliferation by FACS combining Ki67 and Hoechst 33342 staining in WT and Lck$^{-/-}$ cells at 0, 24, 48, and 72 h after N4 peptide stimulation. Representative results from three independent samples are shown. (*B*) Mean percentage of cells in either G0/1, S, or G2/M phase between WT and Lck$^{-/-}$ samples, quantified from the FACS data. (*C*) Representative forward/side scatter plots showing separation of live and dead cell populations at 48 h and 72 h poststimulation. (*D*) Frequency of dead cells in the total cell population ($n \geq 3$). (*E*) The overall proliferation of the populations was calculated using the division index function from FlowJo software. (*F*) Cell recovery from individual cultures at 48 h and 72 h. Error bars correspond to 1 SD of the mean. *$P < 0.05$, **$P < 0.01$, two-tailed *t* test. ns, nonsignificant.

cells and was not restored to N4 levels by addition of exogenous IL-2. By 72 h, however, when continued Myc expression in T cells is largely sustained by cytokine signaling (27, 30), the addition of IL-2 to G4 cells had a significant rescue effect on Myc abundance (Fig. 7*B*). Similarly, fibrillarin and 28S rRNA expression seemed to be driven by TCR signals in the first 24 h of stimulation because their abundance was independent of IL-2 supplementation. By 72 h, in G4-stimulated cultures with exogenous IL-2, fibrillarin (Fig. 7*D*) and 28S rRNA abundance (Fig. 7*E*) were restored to N4 levels ($n = 3$, $P < 0.025$, two-tailed *t* test) whereas both were significantly reduced in G4 cells without addition of IL-2. Lck$^{-/-}$ cells stimulated in N4 peptide possessed a similar requirement for IL-2 to up-regulate Myc and ribosome production and to sustain proliferation at 72 h (Fig. S2).

The results are in agreement with our prior understanding of Myc regulation in T cells, which is driven by TCR signals upon antigen encounter and maintained by IL-2 signaling at later stages (30). It is likely that weakly stimulated T cells are unable to produce sufficient IL-2 to sustain expression of Myc and, consequently, its target genes involved in ribosome biogenesis. In the absence of sufficient ribosome production, T cells fail to expand and survive.

Discussion

This study was undertaken to gain an understanding of the extent to which protein production in CD8 T cells is regulated at the level of translation in response to TCR triggering. We show that weakly activated T cells, while substantially reducing overall translation, also prioritized translation of particular mRNA species over others. That the spectrum of translated mRNAs can be varied in relation to the total rate of protein synthesis has been recognized for many years (33), and specific signaling pathways, such as Ras, Akt, and mTOR, which regulate the function of the mRNA 5′ cap-binding protein eIF4E, have been shown to contribute to this translational discrimination (34–36). Here, we provide a comprehensive analysis of the mRNA species that are subject to translational control after weak stimulation in primary CD8 T cells. We found that a major pathway that showed translational repression after suboptimal TCR triggering was ribosome biogenesis, one of the more energetically costly processes that are undertaken by activated cells (10). We confirmed that weakly stimulated T cells had reduced signaling through both Ras/Erk, Akt, and mTOR and a significant reduction in intracellular ribosomes, as judged by FACS staining for 18S and 28S RNA at 24 h after stimulation. Concomitant with reduced ribosome biogenesis was a failure to sustain the extensive proliferation demonstrated by T cells stimulated with strong agonist antigens.

Primary naive lymphocytes are naturally quiescent, exhibiting very little protein translation despite containing substantial

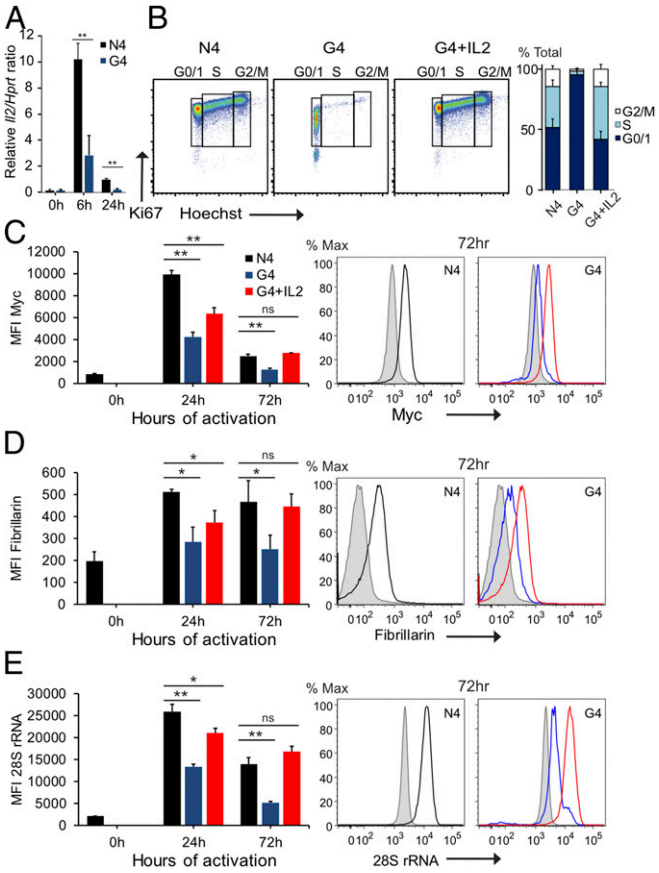

Fig. 7. Exogenous IL-2 sustains proliferation and ribosome biogenesis in G4-stimulated WT cells. (*A*) Relative level of *Il2* transcript in WT-N4 and WT-G4 cells at 0 h, 6 h, and 24 h, measured by qRT-PCR, normalized against *Hprt* level ($n = 4$). (*B*) Cell cycle analysis by FACS in WT-N4, WT-G4, and IL-2–supplemented (20 ng/mL) WT-G4 T cells at 72 h after peptide stimulation. Representative results from three independent samples are shown. (*C–E*) Intracellular level of Myc, fibrillarin, and 28S rRNA, respectively, measured by FACS at 0 h, 24 h, and 72 h post-peptide stimulation. Bar charts represent the mean MFI from three biological replicates. Error bars correspond to 1 SD of the mean. *$P < 0.05$, **$P < 0.01$, two-tailed *t* test. ns, nonsignificant. One representative sample from each group is shown as FACS histograms on the *Right* (gray shaded, 0 h; black solid line, WT-N4 72 h; blue line, WT-G4 72 h; red line, IL2-supplemented WT-G4 72 h).

amounts of mRNA. Analysis of the polysome gradient profile from naive T cells showing the presence of a 48S peak indicated that mRNAs were retained at the preinitiation complex and that joining of the 60S ribosomal subunit to the 48S complex did not take place. This lack of ribosome assembly resulted in few polysomes in naive T cells and little active mRNA translation. Initiation of ribosome biogenesis is an essential first step upon T-cell activation to equip the cell with the machinery necessary to meet the demands of protein synthesis required for proliferation and differentiation. rRNA synthesis in primary lymphocytes has been shown previously to be regulated at the level of ribosomal DNA (rDNA) transcription and mature rRNA decay. Little transcription of rRNA precursors and decay of a high proportion of mature rRNA occur in naive T cells compared with PHA-stimulated cells (37). Here, we showed an additional level of regulation of rRNA synthesis in naive T cells, in which rRNA precursors were accumulated as 30S and 21S species. Activation by TCR engagement generated new ribosomes through a coordinated up-regulation of early pre-rRNA synthesis and rRNA processing. The increase in de novo ribosome synthesis provided sufficient increase in ribosome abundance for efficient polysome formation in OT1 CD8 T cells stimulated with strong agonist peptide. In the absence of Lck, both rRNA transcription and processing were diminished, resulting in a reduced cellular ribosome content. $Lck^{-/-}$ cells did increase translation initiation upon stimulation with N4 peptide, as indicated by reduced 48S and 60S peaks compared with naive T cells. However, a global reduction in subpolysomal peaks and the level of polysome-bound mRNAs in $Lck^{-/-}$ T cells suggested a relatively lower rate of translation initiation, which may have resulted from the combined effect of fewer free ribosomes and a reduction in specific translation factors.

In addition to the overall reduction in translation in $Lck^{-/-}$ T cells, ~24% of all unique expressed probes in the polysome microarray were shown to be specifically down-regulated in their translation compared with WT T cells, indicating that TCR signaling controlled the translation of specific gene subsets. Pathway analysis indicated that a subset of proteins involved in ribosome biogenesis were affected at this level also. Additionally, a number of translationally regulated proteins have been previously shown to regulate translation of specific genes. For example, differences in the abundance of proteins, such as eIF6, between WT and $Lck^{-/-}$ T cells may have influenced the range of mRNA species that are translated. The antiassociation factor eIF6 prevents premature binding of 40S and 60S ribosome subunits (38) and has been shown to affect G1/S cell cycle transition (39, 40) and the expression of metabolic enzymes controlling fatty acid synthesis and glycolysis (41). A G1/S block was observed in $Lck^{-/-}$ cells at 24 h after stimulation, and Kyoto Encyclopedia of Genes and Genomes (KEGG) pathway analysis showed that fatty acid metabolism was highly enriched in the translationally repressed gene subset in $Lck^{-/-}$ cells. Depletion of Tif6 in yeast results in loss of 60S ribosome, which can be rescued by ectopic expression of human eIF6 (42–44), suggesting a possible role of eIF6 in ribosome biogenesis in mammalian cells. eIF6 is also known to regulate translation of a subset of mRNAs containing upstream (u)ORF motifs in their 5′ UTR (41). Overexpression of eIF6 in a murine mast cell line enhanced the production of IL-2 (45), which contains uORF in its transcript (46). The specific down-regulation of eIF6 in $Lck^{-/-}$ cells may result from a combination of multiple signaling defects. eIF6 has been shown to be up-regulated in mast cells by FcεR1 cross-linking and to be inhibited by cyclosporin A (45), and Ca^{2+} signaling is particularly compromised in the absence of Lck in both CD4 (15) and CD8 T cells (47). Additionally, eIF6 promoter activity has been shown to be regulated by GABP (48), an Ets-like transcription factor partially regulated by ERK (49), which is less strongly activated in $Lck^{-/-}$ cells. Whether the translationally regulated gene subsets identified by polysome analysis here are regulated by eIF6 requires further studies involving direct manipulations of the translation factor. So far, we have failed to identify specific enriched sequence motifs on the mRNA of the translationally regulated gene subsets from analyses of the data obtained from the polysome arrays, and the precise contributions of individual ribosomal proteins and translation factors in regulating translation in primary T cells remain to be elucidated.

Of relevance, Lck has been shown to be lost in senescent human T cells, which become refractory to stimulation (21, 22), possibly as a result of being unable to maintain sufficient ribosome biogenesis after stimulation. Of note, heterozygosity of rpS6 (50) and loss of rpL22 (51) have been shown to impede, respectively, peripheral T-cell and αβ DN thymocyte proliferation, through up-regulation of p53 and imposition of a G0/G1 cell cycle block. However, we did not find changes in abundance of RPS6 in $Lck^{-/-}$ T cells nor in many of the other structural ribosomal proteins, which tend to be highly abundantly expressed in T cells (total RNA expression array, GEO accession GSE84781).

We showed that, despite a global reduction in signaling pathway activation in $Lck^{-/-}$ N4-stimulated and WT G4-stimulated T cells, the supplement of exogenous IL-2 was sufficient to restore ribosome abundance, proliferation, and survival at 72 h of culture. STAT5 is activated by IL-2 and has been shown to regulate the expression of various cyclins and CDKs required for cell cycle progression through the G1 and S phases (52). IL-2 signaling is also very important for maintaining Myc translation because Myc protein, but not mRNA, is lost when cytotoxic T cells (CTLs) are incubated with the JAK inhibitor tofacitinib (30, 53). Preston et al. showed that proinflammatory cytokines are required to maintain Myc protein abundance because, in T cells, these cytokines sustain expression of amino acid transporters, which in turn support the amino acid uptake required to replenish rapidly turning over Myc protein (30). Myc coordinates transcription of genes involved in processing of rRNA precursors, ribosome assembly, and nuclear cytoplasmic transport (32), and we showed that one such target involved in pre-rRNA processing, fibrillarin, was coordinately regulated with Myc in weakly stimulated T cells. Together, our data suggest that the maintenance of Myc expression by IL-2 is essential for T cells to maintain ribosome sufficiency and thus proliferation. These data corroborate previously published observations that immunization with weak peptides (3) and viral activation of $Lck^{-/-}$ CD8 T cells (54) inhibit expansion of CD8 T cells rather than activation, per se, or the formation of memory cells.

Much of our current understanding of ribosome biogenesis in eukaryotes has come from studies on yeast model systems and mammalian cell lines. Our data illustrate that CD8 T cells provide a good primary cell model system for studying ribosome biogenesis. Many of the biological processes central to T-cell function are regulated at the level of translation, and ensuring sufficient ribosomal capacity is fundamental to this process.

Materials and Methods

Cell Culture and Stimulation. Lymph node (LN) OT-I T cells were cultured in Iscove's Modified Dulbecco's Medium (IMDM) (Sigma) supplemented with 10% FCS, L-glutamine, 100 U/mL penicillin, 100 U/mL streptomycin, and 50 μM 2-β-mercaptoethanol (2β-ME). We added 100 μM phorbol 12,13-dibutyrate (Sigma), 0.1 μg/mL ionomycin (Sigma), 100 nM SIINFEKL (N4) or 1 μM SIIGFEKL (G4) peptides (Peptide Synthesis) to culture media, and the cells were incubated at 37 °C for the duration specified in each experiment.

Flow Cytometry. For surface marker staining, live cells were labeled with Alexa Fluor 488-, PE-, or PE-Cy7–conjugated mAbs against mouse CD69 (Biolegend), CD25 (BD Biosciences), and CD8b (eBioscience), respectively, for 20 min at 4 °C before fixation in 2% formaldehyde in PBS. For cell activation kinetic experiment, cells were fixed in 2% formaldehyde, followed by intracellular staining using the Phosflow fixation/permeabilization buffers (BD Biosciences) with antibody against pERK1/2 (p44/42-MAPK) Thr202/Tyr204, pRPS6

Ser240/244, and pAkt Thr308 (all Cell Signaling); for cell cycle analysis, fixed-permeabilized cells were stained with Hoechst 33342 (Sigma) and PE-conjugated Ki67 antibody (BD Biosciences). For translation factor analyses, formaldehyde-fixed cells were permeabilized using the eBioscience FoxP3/Transcription Factor Staining Buffer Set and then labeled with antibody against eIF4E and eIF6 (both Cell Signaling). Cells were incubated with primary antibodies for 4 h at 4 °C and washed, followed by staining with goat anti-rabbit Alexa Fluor 647 secondary antibody (Thermo Fisher Scientific) for 1 h at room temperature. All analyses were done on $CD8b^+$ singlet events.

For flow-FISH experiments, naive T cells were labeled with CellTrace Violet Cell Proliferation Kit (Thermo Fisher Scientific) and then activated with peptide antigens in culture for specified durations. Cultured cells were fixed with 2% formaldehyde and then permeabilized in 50% ethanol in PBS at −20 °C. Cells were washed with FACS Buffer (0.5% BSA, 0.01% sodium azide, 2 mM EDTA in PBS) and then hybridized with 5′ Alexa Fluor 488-conjugated oligonucleotide probe against 18S rRNA (TTTACTTCCTCTAGATAGTCAAGTTCGACC) adapted from a previous study (55) or scramble sequence (ACCTTCATTCTCGTAATCCGTTCGAAGTTA) in hybridization buffer (0.9 M NaCl, 20 mM Tris·HCl, pH 7.2, 2 mM EDTA, 0.5% saponin, 20% formamide) for 3 h at 50 °C. At the end of hybridization, cells were washed with hybridization buffer for 20 min at 50 °C and then briefly with ice cold FACS buffer before resuspending in FACS buffer.

All acquisitions were done on a MACSQuant flow cytometer (Miltenyi Biotec).

Protein Extraction and Western Blotting. Cells were lysed in radioimmunoprecipitation assay (RIPA) buffer (Thermo Fisher Scientific) supplemented with a protease inhibitors mixture (Sigma). The lysates were centrifuged to remove the debris, and total protein in the supernatants was quantitated using a Pierce BCA Protein Assay Kit (Thermo Fisher Scientific). Reducing sample buffer was added to the lysates, and samples were heated to 95 °C and separated by SDS/PAGE. Proteins were transferred to an Immobilon-FL PVDF membrane (Millipore), and membranes were incubated in Odyssey blocking buffer (LI-COR Biosciences) before incubation with the primary antibodies. Quantitative signals were generated with secondary Abs: anti-rabbit IRDye 800CW (LI-COR Biosciences) and anti-mouse Alexa Fluor 680 (Thermo Fisher Scientific) and visualized using the Odyssey Infrared Imaging System (LI-COR Biosciences).

The following primary Abs were used: anti-Zap70 (BD Biosciences); anti-RPS7, RPL4, fibrillarin, and eIF4A2 (all Abcam); and anti-RPS6, eIF2α, eIF4E, eIF6, and eEF2 (all Cell Signaling). Secondary Abs were as follows: anti-rabbit IRDye 800CW (LI-COR Biosciences) and anti-mouse Alexa Fluor 680 (Thermo Fisher Scientific).

Sucrose Gradient Fractionation and Polysome Analysis. Methods were adapted and modified from a previous study (56). Cycloheximide (Sigma) was added to the media at 100 μg/mL for 10 min at 37 °C at the end of the culture. The cells were harvested and lysed in gradient buffer (300 mM NaCl, 15 mM $MgCl_2$, 15 mM Tris·HCl, pH 7.5, 2 mM DTT, 100 μg/mL cycloheximide) supplemented with 1% Triton X-100, 0.5 U/μL RNase inhibitor (Promega), and a mixture of protease inhibitors (Sigma). Postnuclear supernatants were loaded onto 10 to 50% sucrose step gradients in gradient buffer and separated by centrifugation at 38,000 rpm for 2 h at 4 °C in an SW-40 rotor (Beckman Coulter). RNA content was read across the gradients through a live 254-nm UV spectrometer (Isco), and each sample was collected in 10 fractions. Fraction 1 to 5 were pooled and define as the subpolysomal fraction whereas fraction 6 to 10 were pooled and defined as the polysomal fraction. To make polysome profiles directly comparable between samples in a batch of experiment, total ribonuclear protein was extracted from the same cell number, lysates were loaded into sucrose gradient columns made in the same batch, and OD readings were taken with the same machine setting on the same day. The baseline in each sample was determined by the lowest OD value within the profile. Total RNA was extracted from the pooled fractions using TRIzol reagent (Thermo Fisher Scientific) and further purified with acid phenol-chloroform and ethanol precipitation.

RNA Extraction and Pre-rRNA Northern Blotting. The experimental procedure was adapted from a previous publication (56). Total RNA was extracted from cells using an RNeasy kit (Qiagen) supplemented with 5×10^{-5} M 2β-ME during the lysing step. Samples were separated on 1% agarose-formaldehyde-Mops gels and then transferred onto a Hybond-XL membrane (Thermo Fisher Scientific) in 20× SSC (Thermo Fisher Scientific). After cross-linking of RNA on the membranes using a 254-nm Stratalinker, the membranes were incubated in Church and Gilbert's buffer (180 mM Na_2HPO_4, 70 mM NaH_2PO_4, 7% SDS) for 30 min at 55 °C. Then, 50 pmol of oligonucleotide probe (Thermo Fisher Scientific) was labeled with [γ-^{32}P]ATP (Perkin-Elmer) using T4 polynucleotide kinase (New England Biosciences) and purified using a G25 column (GE Healthcare). The probe was hybridized with the membranes overnight (16 h) at 55 °C, and the membranes were washed with 4× SSC and then 2× SSC at room temperature. Autoradiography was performed using a phosphorscreen, and signals were acquired using a Typhoon Trio phosphorimager and analyzed with ImageQuant TL software (all GE Healthcare). Probe sequences were individually adopted from previous studies: ITS-1-mus (GCTCCTCCACAGTCTCCCGTTAATGATC) (55) and ITS-2-mus (ACCCACCGCAGCGGGTGACGCGATTGATCG) (57).

Transcription and Translation Analyses by RT-qPCR. Total cellular RNA and polysomal/subpolysomal RNA were reverse-transcribed using SuperScript III enzyme (Thermo Fisher Scientific) with oligo$(dT)_{18}$ Primer. qPCR was performed on a Light Cycler 480 (Roche) using Brilliant III SYBR Master Mixes (Agilent). The transcription level of each gene was normalized against the quantity of *Hprt* in the sample ($n = 3$, two-tailed t test); translation was determined by measuring the mRNA abundance in the polysomal fraction normalized against that in the subpolysomal fraction in each sample ($n = 4$, $^*P < 0.05$, two-tailed t test); total protein (surface plus intracellular) was quantified by FACS analysis of fixed and permeabilized cells using specific Abs ($n = 7$, $^{**}P < 0.01$, two-tailed t test).

^{32}P Orthophosphate Autoradiography. The procedure was adapted from a previous publication (56). For naive T cells, ^{32}P orthophosphate was added to the media to a final concentration of 20 μCi/mL, and the cells were cultured for 1 h before being stimulated with the SIINFEKL peptide. Cells were harvested just before adding the peptide, and 0.5 h, 1 h, 2 h, 4 h, and 8 h after the stimulation. For activated cells, ^{32}P orthophosphate was added to the cell culture and then washed off after 1 h of incubation. Cell pellets were taken at 0 h, 1 h, 2 h, and 4 h after labeling. Total RNA extraction, gel electrophoresis, capillary transfer, and autoradiography were performed as described above for Northern blotting procedure.

Analysis of Microarray Data. GenePix Pro-6.0 was used to quantify fluorescence intensities for individual spots on the microarray. All statistical analyses were performed in the statistical environment R, version 2.6.1 and the Limma (58), RankProd (59), and Siggenes (60) packages. Briefly, raw intensities for both channels (Cy5 Polysomal RNA and Cy3 Subpolysomal RNA) were background-corrected and normalized by scaling. Dye-swapped samples were averaged to correct for bias. Each $Lck^{-/-}$ mouse condition was compared individually with the WT mouse condition using data from four biological repeats. Expressed genes were selected based on an artificially set threshold for the average signal intensity of the corresponding probe(s), defined as 1.1× the 95th percentile of the negative controls. Differentially expressed genes were then identified using the RankProd test.

ACKNOWLEDGMENTS. This work was funded by Wellcome Trust Investigator Award WT096669AIA (to R.Z.).

1. Kay JE (1968) Early effects of phytohaemagglutinin on lymphocyte RNA synthesis. *Eur J Biochem* 4:225–232.
2. Yoon H, Kim TS, Braciale TJ (2010) The cell cycle time of CD8+ T cells responding in vivo is controlled by the type of antigenic stimulus. *PLoS One* 5:e15423.
3. Zehn D, Lee SY, Bevan MJ (2009) Complete but curtailed T-cell response to very low-affinity antigen. *Nature* 458:211–214.
4. Anderson P (2010) Post-transcriptional regulons coordinate the initiation and resolution of inflammation. *Nat Rev Immunol* 10:24–35.
5. Scheu S, et al. (2006) Activation of the integrated stress response during T helper cell differentiation. *Nat Immunol* 7:644–651.
6. Sandberg R, Neilson JR, Sarma A, Sharp PA, Burge CB (2008) Proliferating cells express mRNAs with shortened 3′ untranslated regions and fewer microRNA target sites. *Science* 320:1643–1647.
7. Moss T, Langlois F, Gagnon-Kugler T, Stefanovsky V (2007) A housekeeper with power of attorney: The rRNA genes in ribosome biogenesis. *Cell Mol Life Sci* 64:29–49.
8. Grummt I (2003) Life on a planet of its own: Regulation of RNA polymerase I transcription in the nucleolus. *Genes Dev* 17:1691–1702.
9. Thomson E, Ferreira-Cerca S, Hurt E (2013) Eukaryotic ribosome biogenesis at a glance. *J Cell Sci* 126:4815–4821.
10. Granneman S, Tollervey D (2007) Building ribosomes: Even more expensive than expected? *Curr Biol* 17:R415–R417.
11. Johnson LF, Abelson HT, Green H, Penman S (1974) Changes in RNA in relation to growth of the fibroblast. I. Amounts of mRNA, rRNA, and tRNA in resting and growing cells. *Cell* 1:95–100.
12. Hukelmann JL, et al. (2016) The cytotoxic T cell proteome and its shaping by the kinase mTOR. *Nat Immunol* 17:104–112.

13. Hanke JH, et al. (1996) Discovery of a novel, potent, and Src family-selective tyrosine kinase inhibitor: Study of Lck- and FynT-dependent T cell activation. *J Biol Chem* 271: 695–701.
14. Straus DB, Weiss A (1992) Genetic evidence for the involvement of the lck tyrosine kinase in signal transduction through the T cell antigen receptor. *Cell* 70:585–593.
15. Lovatt M, et al. (2006) Lck regulates the threshold of activation in primary T cells, while both Lck and Fyn contribute to the magnitude of the extracellular signal-related kinase response. *Mol Cell Biol* 26:8655–8665.
16. Legname G, et al. (2000) Inducible expression of a p56Lck transgene reveals a central role for Lck in the differentiation of CD4 SP thymocytes. *Immunity* 12:537–546.
17. Seddon B, Legname G, Tomlinson P, Zamoyska R (2000) Long-term survival but impaired homeostatic proliferation of Naïve T cells in the absence of p56lck. *Science* 290: 127–131.
18. Zhang B, Kirov S, Snoddy J (2005) WebGestalt: An integrated system for exploring gene sets in various biological contexts. *Nucleic Acids Res* 33:W741–748.
19. Wang J, Duncan D, Shi Z, Zhang B (2013) WEB-based GEne SeT AnaLysis Toolkit (WebGestalt): Update 2013. *Nucleic Acids Res* 41:W77–83.
20. Sloan KE, et al. (2013) Both endonucleolytic and exonucleolytic cleavage mediate ITS1 removal during human ribosomal RNA processing. *J Cell Biol* 200:577–588.
21. Pawelec G, Hirokawa K, Fülöp T (2001) Altered T cell signalling in ageing. *Mech Ageing Dev* 122:1613–1637.
22. Ye J, et al. (2014) TLR8 signaling enhances tumor immunity by preventing tumor-induced T-cell senescence. *EMBO Mol Med* 6:1294–1311.
23. Madrenas J, Chau LA, Smith J, Bluestone JA, Germain RN (1997) The efficiency of CD4 recruitment to ligand-engaged TCR controls the agonist/partial agonist properties of peptide-MHC molecule ligands. *J Exp Med* 185:219–229.
24. Stefanová I, et al. (2003) TCR ligand discrimination is enforced by competing ERK positive and SHP-1 negative feedback pathways. *Nat Immunol* 4:248–254.
25. Stepanek O, et al. (2014) Coreceptor scanning by the T cell receptor provides a mechanism for T cell tolerance. *Cell* 159:333–345.
26. Daniels MA, et al. (2006) Thymic selection threshold defined by compartmentalization of Ras/MAPK signalling. *Nature* 444:724–729.
27. Lord JD, McIntosh BC, Greenberg PD, Nelson BH (2000) The IL-2 receptor promotes lymphocyte proliferation and induction of the c-myc, bcl-2, and bcl-x genes through the trans-activation domain of Stat5. *J Immunol* 164:2533–2541.
28. Chow C-W, Rincón M, Davis RJ (1999) Requirement for transcription factor NFAT in interleukin-2 expression. *Mol Cell Biol* 19:2300–2307.
29. Jain J, Valge-Archer VE, Rao A (1992) Analysis of the AP-1 sites in the IL-2 promoter. *J Immunol* 148:1240–1250.
30. Preston GC, et al. (2015) Single cell tuning of Myc expression by antigen receptor signal strength and interleukin-2 in T lymphocytes. *EMBO J* 34:2008–2024.
31. Schlosser I, et al. (2003) A role for c-Myc in the regulation of ribosomal RNA processing. *Nucleic Acids Res* 31:6148–6156.
32. van Riggelen J, Yetil A, Felsher DW (2010) MYC as a regulator of ribosome biogenesis and protein synthesis. *Nat Rev Cancer* 10:301–309.
33. Lodish HF (1974) Model for the regulation of mRNA translation applied to haemoglobin synthesis. *Nature* 251:385–388.
34. Mamane Y, et al. (2004) eIF4E–from translation to transformation. *Oncogene* 23: 3172–3179.
35. Hara K, et al. (1997) Regulation of eIF-4E BP1 phosphorylation by mTOR. *J Biol Chem* 272:26457–26463.
36. Rajasekhar VK, et al. (2003) Oncogenic Ras and Akt signaling contribute to glioblastoma formation by differential recruitment of existing mRNAs to polysomes. *Mol Cell* 12:889–901.
37. Cooper HL (1970) Control of synthesis and wastage of ribosomal RNA in lymphocytes. *Nature* 227:1105–1107.
38. Gartmann M, et al. (2010) Mechanism of eIF6-mediated inhibition of ribosomal subunit joining. *J Biol Chem* 285:14848–14851.
39. Gandin V, et al. (2008) Eukaryotic initiation factor 6 is rate-limiting in translation, growth and transformation. *Nature* 455:684–688.
40. Ricciardi S, et al. (2015) Eukaryotic translation initiation factor 6 is a novel regulator of reactive oxygen species-dependent megakaryocyte maturation. *J Thromb Haemost* 13:2108–2118.
41. Brina D, et al. (2015) eIF6 coordinates insulin sensitivity and lipid metabolism by coupling translation to transcription. *Nat Commun* 6:8261.
42. Sanvito F, et al. (1999) The β4 integrin interactor p27(BBP/eIF6) is an essential nuclear matrix protein involved in 60S ribosomal subunit assembly. *J Cell Biol* 144:823–837.
43. Si K, Maitra U (1999) The Saccharomyces cerevisiae homologue of mammalian translation initiation factor 6 does not function as a translation initiation factor. *Mol Cell Biol* 19:1416–1426.
44. Wood LC, Ashby MN, Grunfeld C, Feingold KR (1999) Cloning of murine translation initiation factor 6 and functional analysis of the homologous sequence YPR016c in Saccharomyces cerevisiae. *J Biol Chem* 274:11653–11659.
45. Oh CK, Filler SG, Cho SH (2001) Eukaryotic translation initiation factor-6 enhances histamine and IL-2 production in mast cells. *J Immunol* 166:3606–3611.
46. Thierry-Mieg D, Thierry-Mieg J (2006) AceView: A comprehensive cDNA-supported gene and transcripts annotation. *Genome Biol* 7:1–14.
47. Filby A, et al. (2007) Fyn regulates the duration of TCR engagement needed for commitment to effector function. *J Immunol* 179:4635–4644.
48. Donadini A, et al. (2006) GABP complex regulates transcription of eIF6 (p27BBP), an essential trans-acting factor in ribosome biogenesis. *FEBS Lett* 580:1983–1987.
49. Hoffmeyer A, et al. (1998) The GABP-responsive element of the interleukin-2 enhancer is regulated by JNK/SAPK-activating pathways in T lymphocytes. *J Biol Chem* 273:10112–10119.
50. Sulic S, et al. (2005) Inactivation of S6 ribosomal protein gene in T lymphocytes activates a p53-dependent checkpoint response. *Genes Dev* 19:3070–3082.
51. Anderson SJ, et al. (2007) Ablation of ribosomal protein L22 selectively impairs alphabeta T cell development by activation of a p53-dependent checkpoint. *Immunity* 26:759–772.
52. Moriggl R, et al. (1999) Stat5 is required for IL-2-induced cell cycle progression of peripheral T cells. *Immunity* 10:249–259.
53. Akiyama M, et al. (2011) Erythropoietin activates telomerase through transcriptional and posttranscriptional regulation in human erythroleukemic JAS-REN-A cells. *Leuk Res* 35:416–418.
54. Tewari K, Walent J, Svaren J, Zamoyska R, Suresh M (2006) Differential requirement for Lck during primary and memory CD8+ T cell responses. *Proc Natl Acad Sci USA* 103:16388–16393.
55. Rouquette J, Choesmel V, Gleizes PE (2005) Nuclear export and cytoplasmic processing of precursors to the 40S ribosomal subunits in mammalian cells. *EMBO J* 24: 2862–2872.
56. Knight JR, et al. (2016) Cooling-induced SUMOylation of EXOSC10 down-regulates ribosome biogenesis. *RNA* 22:623–635.
57. Ge J, et al. (2010) Dyskerin ablation in mouse liver inhibits rRNA processing and cell division. *Mol Cell Biol* 30:413–422.
58. Smyth GK, Speed TP (2003) Normalization of cDNA microarray data. *Methods* 31: 265–273.
59. Breitling R, Armengaud P, Amtmann A, Herzyk P (2004) Rank products: A simple, yet powerful, new method to detect differentially regulated genes in replicated microarray experiments. *FEBS Lett* 573:83–92.
60. Schwender H (2012) *siggenes: Multiple testing using SAM and Efron's empirical Bayes approaches*. R package version 1.42.0.